J. Fluid Mech. (1978), *vol.* 88, *part* 3, *pp.* 431–449
Printed in Great Britain

The turbulent concentration field of a methane jet

By A. D. BIRCH, D. R. BROWN, M. G. DODSON AND J. R. THOMAS

British Gas Corporation, Research and Development Division, Midlands Research Station, Wharf Lane, Solihull, West Midlands, England B91 2JW

(Received 11 October 1977)

Detailed measurements of turbulent concentration parameters in a round free methane jet up to 70 diameters downstream from the jet source are described. The concentration changes were obtained using a Raman spectrometer designed for the measurement of a methane vibrational transition function, and processed using a photon correlator. Mean and fluctuating concentration levels are given, together with the concentration probability density distribution.

A theory for interpreting the statistical aspects of the signal is presented and results are compared with other data from the literature on jets of uniform and non-uniform density. It is shown that the intensity of concentration fluctuations has an asymptotic value of 28·5 % in the far field region of the jet. One interesting feature of the data is the deviation from Gaussian statistics along the jet centre-line.

1. Introduction

An important aspect associated with the formation of turbulent reacting systems is the way in which the temporal qualities of the flow affect the rate and extent to which combustible mixture is produced. One feature which is often of particular interest is the level of fluctuation of composition about some average value. Although a considerable number of investigations of fluctuating velocity fields have been made (Wygnanski & Fiedler 1969; Ribeiro & Whitelaw 1974), far less information is available on the relevant scalar parameters. Long (1963) and Field *et al.* (1967) have given comprehensive reviews of measurements of velocity and concentration in a round free jet, and this earlier work established the hyperbolic nature of the mean parameters, especially in the near field. More recent work by Antonia, Prabhu & Stephenson (1975) and Venkataramani, Tutu & Chevray (1975) on the temperature field in heated jets has provided information on some of the higher moments of the probability density function in the far field. In the case of concentration measurements employing sampling probe techniques this information is less readily available, although oil fog light scattering techniques have been used to evaluate concentration fluctuations in air jets (Becker, Hottel & Williams 1967).

In this paper we describe an investigation into the transfer of concentration in a turbulent free jet of natural gas using a novel technique based on Raman scattering of laser light. The Raman effect arises when light interacts with the electromagnetic field of a molecule, leading to the scattering of photons with a different frequency from that of the incident light. Whether or not a particular substance exhibits Raman activity depends on certain criteria known as selection rules; for example a condition for vibrational Raman activity is that the molecular polarizability must change during

inter-nuclear stretching. Since the Raman shift in frequency is determined by an internal energy transition, it is characteristic of the particular species concerned. The transition probability and hence the intensity of Raman scattered light can be shown to be linearly proportional to the number density of the scattering molecules, which under isothermal conditions is equivalent to concentration by volume. A particular advantage of this method is that no significant perturbation is produced within the system under investigation, and concentration is measured directly. Furthermore, the scattered light can be collected from a small region of a laser beam, thus giving good spatial resolution.

Earlier work on laser Raman spectroscopy (Hartley 1974; Widhopf & Lederman 1971) seemed to indicate that extremely high laser powers were necessary even to achieve measurements of mean concentration. However, we have found that with relatively modest laser powers, the use of photon correlation methods enables information on mean and fluctuating concentration to be extracted (Birch *et al.* 1975*a*). This approach has been developed and extended in this paper so that it has now been used to obtain the higher-order moments of the probability distribution as well as the mean, r.m.s. and power spectrum of the fluctuations in a round free jet of natural gas.

An interesting feature of the results is the observation that the skewness is highly negative at the axis of symmetry, compared with the corresponding velocity moment. In addition, the far field fluctuation intensity is exceeded everywhere by the local velocity fluctuation intensity. Results are also presented on the macro scale of turbulence by combining the velocity information obtained using a laser anemometer (Birch *et al.* 1975*b*) and the correlation time (Taylor's hypothesis). These results show reasonable agreement with those of Becker *et al.* (1967) and Shaughnessy & Morton (1977) for air jets.

2. Theory

In this section the nature of the detected Raman signal produced by a fluctuating concentration level in the fluid is considered, and equations are developed which allow statistical information about the concentration field to be extracted.

As the Raman effect is very weak in gases, a photon counting technique has been used to measure the scattered light intensity. This introduces the Poisson statistics of the photoelectric effect, and the fluctuations in the recorded photodetections may be regarded as arising from two sources:

(*a*) the random ejection of photoelectrons even when there are no fluctuations in the light intensity, I, falling on the detector surface, and

(*b*) the fluctuations in the incident light intensity because of temporal variations in molecular number density at the sampling location.

The probability $p(n, T)$ that n electrons will be released during a time interval T at a photocathode because of a normally incident light beam is related to the probability density P for the integrated light intensity W by the equation (Mandel 1959; Meltzer & Mandel 1970):

$$p(n,T) = \frac{1}{n!}\int_0^\infty (\epsilon W)^n \exp\{-\epsilon W\} P(W)\, dW, \tag{1}$$

where

$$W = \int_t^{t+T} I(t)\, dt,$$

and ϵ is the quantum efficiency of the detector. This equation shows that the photocounting probability $p(n, T)$ is obtained by averaging a Poisson distribution with parameter ϵW over the incident field ensemble. The problem of formally determining $P(W)$ from a measurement of $p(n, T)$ has been examined by Bédard (1967), who inverted (1) in terms of Laguerre polynomials. Unfortunately, it appears that this method is restricted to analytical expressions for the photocount distribution, and is thus unsuitable for experimental data. Information on $P(W)$ can, however, be extracted in the form of the integral moments (Pike 1969), in the following way. The factorial moments of $p(n, T)$, defined as

$$n_s = \sum_{n=0}^{\infty} n(n-1)(n-2)\dots(n-s+1)\,p(n, T), \tag{2}$$

can be related to the moments about the origin of $P(W)$ by

$$n_s = \int_0^{\infty} W^s P(W)\,dW. \tag{3}$$

Let Q be the time average probability density function of concentration, η (expressed in volume fraction terms). Then the linear relationship between W and η allows Q to be specified by a simple transformation of P,

$$Q(\eta) = KTP(W), \tag{4}$$

where K is the Raman count rate when the concentration of scattering fluid in the sample volume is unity. If b is the background count rate, caused mainly by stray light, then

$$n_s = (KT)^s \int_0^1 (\eta + b/K)^s Q(\eta)\,d\eta, \tag{5}$$

and the jth central moment of $Q(\eta)$ can be written as

$$\mu_j = (KT)^{-j} \sum_{s=0}^{j} \frac{j!}{s!\,(j-s)!} (-n_1)^s n_{j-s}, \tag{6}$$

for $j \geqslant 2$. The mean concentration $\bar{\eta}$ is given by

$$\bar{\eta} = (n_1 - bT)/KT. \tag{7}$$

A complementary method, which provides spectral information, has previously been reported (Birch *et al.* 1975*a*), where the photon correlation function $G(\tau)$ was shown to be

$$G(\tau) = A\{\tilde{\eta}^2 K^2 R(\tau) + (K\bar{\eta} + b)^2\}, \tag{8}$$

for $\tau \neq 0$. (A is a constant, $R(\tau)$ is the normalized autocorrelation function of the concentration fluctuations and $\tilde{\eta}$ is the root-mean-square concentration.) An independent determination of $\bar{\eta}$ enables $\tilde{\eta}$ and $R(\tau)$ to be separated provided that the point at infinity is known. The power spectral density, $E(\nu)$, can then be obtained by a Fourier cosine transformation of the autocorrelation:

$$E(\nu) = 4 \int_0^{\infty} R(\tau) \cos 2\pi\nu\tau\,d\tau, \tag{9}$$

the integration being accomplished using Filton's method.

The above analysis is concerned with concentration expressed in volume fraction terms. Later on in the text it will be necessary to employ the mass fraction definition θ. These two methods of specifying concentration are, at every instant of time, uniquely related in a binary mixture by:

$$\theta = (\alpha+1)\,\eta/(\alpha\eta+1), \tag{10}$$

where

$$\alpha = \rho_0/\rho_a - 1,$$

and ρ_0, ρ_a are the densities of the fluid and diluent respectively. However, any time average relationships between the two parameters must account for the turbulent fluctuations superimposed on the mean values. Denoting the instantaneous values of θ and η as follows:

$$\theta = \bar{\theta} + \theta', \quad \eta = \bar{\eta} + \eta',$$

and substituting into (10) and expanding binomially:

$$\bar{\theta} + \theta' = \frac{\alpha+1}{\alpha}\left\{\frac{\alpha\bar{\eta}}{\alpha\bar{\eta}+1} - \frac{1}{\alpha\bar{\eta}+1}\sum_{j=1}^{\infty}\left(\frac{-\alpha\eta'}{\alpha\bar{\eta}+1}\right)^j\right\}. \tag{11}$$

Time averaging (11) produces

$$\bar{\theta} = \frac{(\alpha+1)\,\bar{\eta}}{\alpha\bar{\eta}+1} - \frac{(\alpha+1)}{\alpha(\alpha\bar{\eta}+1)}\sum_{j=2}^{\infty}\left(\frac{-\alpha}{\alpha\bar{\eta}+1}\right)^j \mu_j, \tag{12}$$

and

$$\theta' = \frac{(\alpha+1)\,\eta'}{(\alpha\bar{\eta}+1)^2} + \frac{(\alpha+1)}{\alpha(\alpha\bar{\eta}+1)}\sum_{j=2}^{\infty}\left(\frac{-\alpha}{\alpha\bar{\eta}+1}\right)^j \{\mu_j - \eta'^j\}. \tag{13}$$

It can be seen that a complete knowledge of the probability $Q(\eta)$ is required for the exact transformation into mass fraction. In the present work (12) was used up to fourth order, in η'. The error in mean concentration caused by this truncation was $\ll 1\,\%$. The maximum error which would have resulted from using only the first term of (12) was found to be approximately 4 %. If (13) is terminated after the first order in fluctuating quantities, it follows that the r.m.s. mass fraction concentration, $\tilde{\theta}$, is given by

$$\tilde{\theta} \simeq (\alpha+1)\,\tilde{\eta}/(\alpha\bar{\eta}+1)^2. \tag{14}$$

It was again found that the use of this expression led to an error of $< 1\,\%$ compared with the inclusion of higher terms. Also, since θ' can be taken to be a linear function of η', the higher moments of the probability distributions, when suitably normalized by powers of the variance, are equivalent. Similar considerations show that, to this level of approximation, the autocorrelation functions for the two concentration units are identical.

3. Experimental

The flow system consisted of a free isothermal natural gas jet (approx. 95 % methane) issuing from a 12·65 mm diameter tube with a length to diameter ratio of 50, the Reynolds number of the flow being 16 000. The velocity profile at the origin was typical of fully developed pipe flow, being well described by a $\frac{1}{7}$th power law. The displacement thickness was 0·636 mm and the associated shape factor was 1·317. The jet could be accurately positioned to within $\pm 0{\cdot}1$ mm with respect to the laser beam by three-dimensional traversing equipment using lead screws and stepper motors.

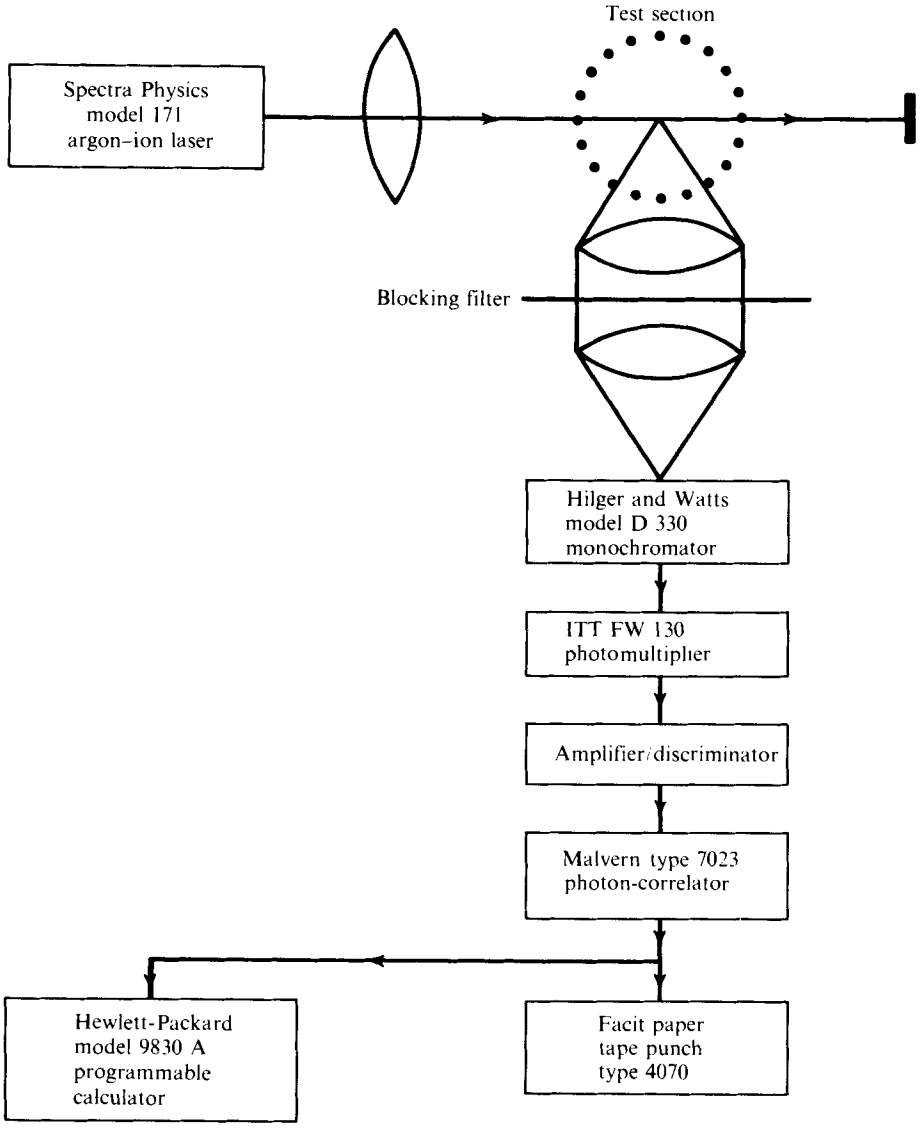

FIGURE 1. Laser Raman system for concentration measurements.

The experimental apparatus consisted of a laser Raman system for measuring species concentration, used in conjunction with a laser anemometer for velocity measurements. An overall configuration of the Raman system is shown in figure 1. The light source was a Spectra Physics 171 continuous wave argon-ion laser, operating at 488 nm with an output power of 4 Watts, the beam being focused to a waist diameter of approximately 0·2 mm. Light scattered over a solid angle of 0·08 steradian was collected by a lens system, passed through a blocking filter with a sharp cut-off at 550 nm, and imaged onto the entrance slit of a Hilger and Watts D330 monochromator. The optics were specially coated to reduce reflexion losses at the operating wavelength, and were carefully arranged so that the collected light just filled the mirrors and grating of the monochromator. This was adjusted to select the

Stokes Raman band of methane, corresponding to a transition from the ground to first excited vibrational state located at 2917 wavenumbers from the exciting line (i.e. at 569 nm). This radiation was detected by a cooled ITT FW 130 photomultiplier tube, having a high quantum efficiency (9·7 % at 569 nm) and giving less than one dark count per second at −25 °C, the output was fed into a discriminator/amplifier and then processed by a Malvern Instruments K7023 photon correlator (see Jakeman 1973). The correlator could be used in (*a*) autocorrelation mode to give the photon correlation function of the signal, or (*b*) probability mode to give an unnormalized version of the photon count probability function $p(n, T)$.

The system was calibrated by measuring the count rate when 100 % natural gas was present in the sample volume, and subtracting the background signal, b (obtained when no natural gas was present), to give the sensitivity factor K. The gas concentration corresponding to any particular measured signal could then be obtained by linear interpolation. With scattered light collected over 0·08 steradians from 2 mm of the incident beam a signal of 1×10^5 counts s^{-1} could be obtained.

An estimate was made of the theoretically expected signal level using the equation given by Tobin (1971)

$$W = TN\sigma\Omega I_0 LC. \tag{15}$$

Here T is the measurement time, N is the molecular number density and L the length of the sample volume; σ, I_0 and Ω refer to the absolute Raman scattering cross-section, the incident light intensity and the solid angle of collection respectively. The transmission loss coefficient C is made up of the product of transmission factors from optical surfaces, monochromator, filters and photomultiplier quantum efficiency, and was estimated to be 0·007. The number density of molecules was calculated to be $2{\cdot}5 \times 10^{25}\,m^{-3}$ at N.T.P.; using data by Fenner *et al.* (1973) for the absolute Raman scattering cross-section ($4 \times 10^{-34}\,m^2$ molecule^{-1} ster^{-1} at 488 nm), the calculation gives an estimated total signal of $1{\cdot}3 \times 10^5$ counts s^{-1} for 100 % methane. The difference between this value and the experimental observation may be due to uncertainties in the assumed cross-section data and the estimated loss coefficient.

Velocity measurements were taken with a laser anemometer consisting of an RCA-LD2186 helium–cadmium laser (operating at 441·6 nm), an EMI photomultiplier tube and photon correlator. Full details of the method and the analysis of the scattered light signal in this case are given elsewhere (Birch *et al.* 1975*b*).

4. Results

4.1. *General features of the turbulent concentration field*

A convenient way of examining the general features of the scalar field is to form the autocorrelation function of the concentration fluctuations, as defined in (8). It was found that in a major part of the flow field this function could be accurately described by a single decaying exponential,

$$R(\tau) = \exp\{-\tau/\mathscr{T}\}, \tag{16}$$

where $\mathscr{T}$ represents the Eulerian integral time scale. It is interesting that a similar function is commonly used to specify the longitudinal spatial correlation and Eulerian autocorrelation for velocity fluctuations (Hinze 1959), subject to the obvious limitations near the vertex. An example of such a correlogram (obtained at an axial location

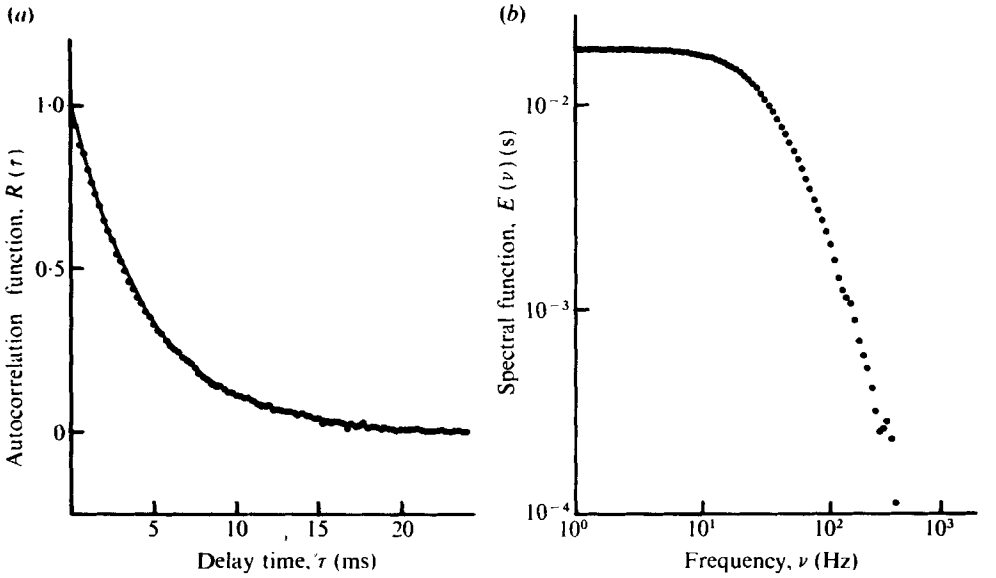

FIGURE 2. (*a*) Autocorrelation function and (*b*) power spectral density function ($z/d = 5{\cdot}7$, $r/d = 1{\cdot}7$).

of $z = 5{\cdot}7$ diameters and radial position of $r = 1{\cdot}7$ diameters) is shown in figure 2(*a*) together with the corresponding power spectral density function (figure 2(*b*)), obtained by Fourier transformation (9). The solid line in figure 2(*a*) shows (16) with $\mathscr{T} = 4{\cdot}55$ ms. This type of correlation function corresponds to random turbulent fluctuations with no dominant frequency. In contrast, the correlogram shown in figure 3(*a*) ($z/d = 0{\cdot}1$, $r/d = 0{\cdot}5$, where d is the orifice diameter) exhibits a distinct periodic component, giving rise to a peak in the spectrum (figure 3(*b*)), indicating that a regular oscillation is superimposed on the random fluctuations at this position. These correlograms could be described accurately by the following equation:

$$R(\tau) = B\exp\{-\nu_1\tau\} + (1-B)\exp\{-\nu_2\tau\}\cos 2\pi\nu_3\tau, \tag{17}$$

where the parameters ν_1 to ν_3 and B were determined from the data by a least squares estimation. This function is shown as a solid line in figure 3(*a*); the value for the periodic frequency ν_3 in this case was 1050 Hz, which corresponds to the peak in the spectrum. This regular flow structure was only observed in a small region close to the lip of the orifice, and is attributed to eddy shedding, the Strouhal number (given by $\nu_3 d/\bar{q}_0$, where $\bar{q}_0$ is the mean exit velocity) being 0·52. A similar feature has also been observed by Grant, Jones & Rosenfeld (1973) using a hot-wire technique. They found that such oscillations occurred with maximum amplitude at this Strouhal number.

The normalized central moments of the probability density distribution of concentration were obtained from the measured $p(n, T)$ functions as detailed in § 2. The method assumes that the photodetection system obeys Poisson statistics; this was tested by measuring the photon count distribution in the potential core of the jet. Here no air has been entrained and, hence, no fluctuations in concentration are possible. The measured r.m.s. and skewness agreed with the Poisson values to better than 1 %. In general, the second moment obtained by the $p(n, T)$ method agreed to within 3 % of the value produced from an autocorrelation experiment, except in

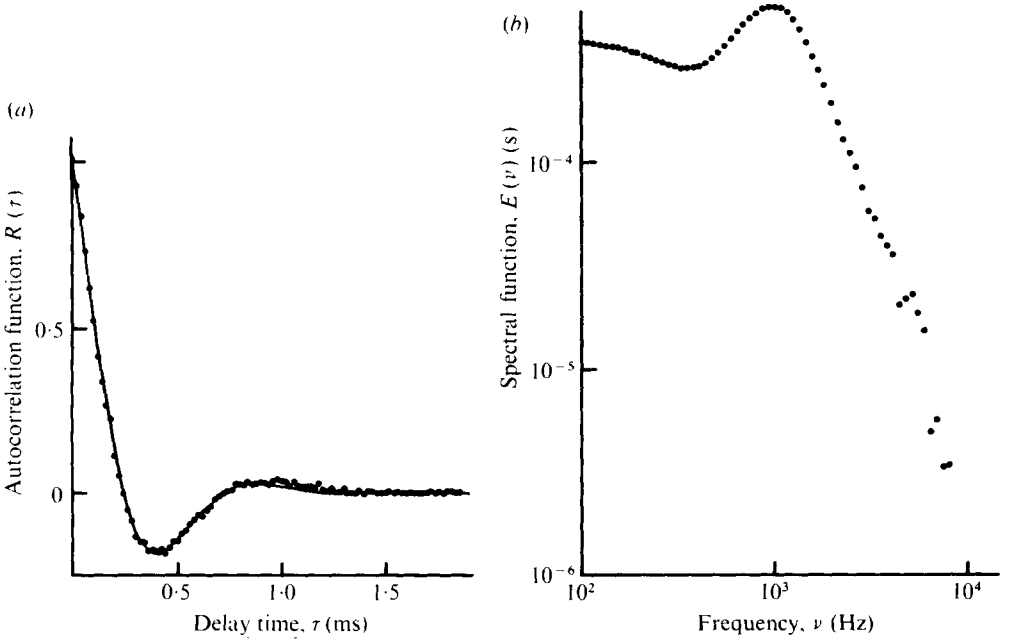

FIGURE 3. (*a*) Autocorrelation function and (*b*) power spectral density function ($z/d = 0{\cdot}1$, $r/d = 0{\cdot}5$).

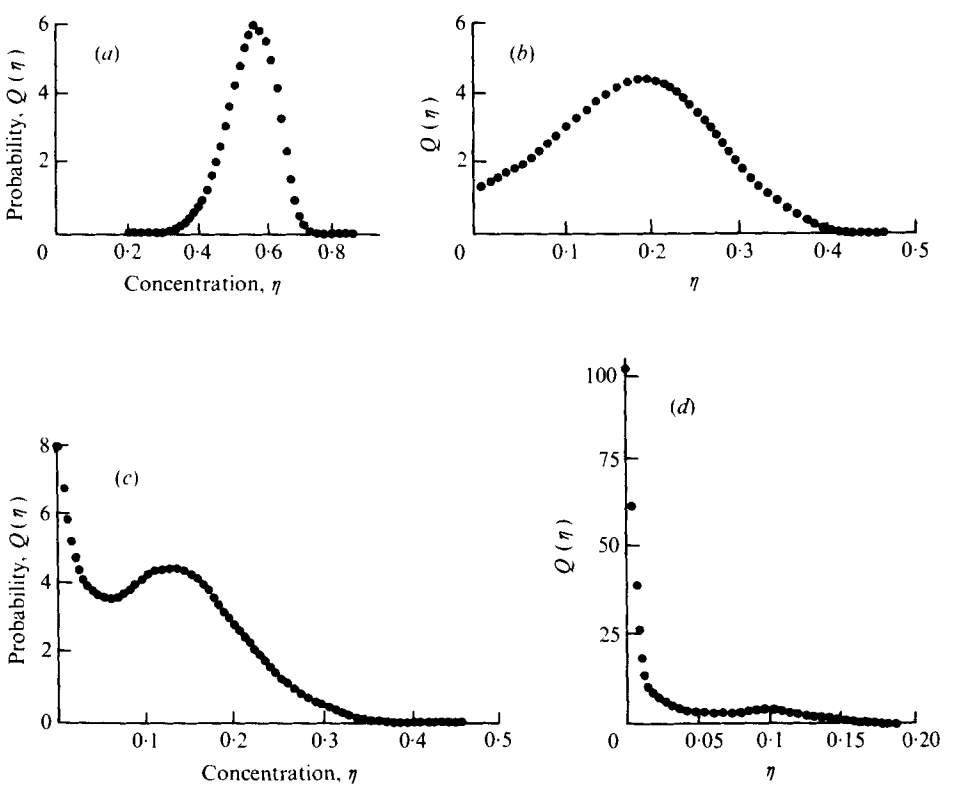

FIGURE 4. Probability distribution of concentration at various radial locations ($z/d \sim 10$). (*a*) $r/d = 0$, $\bar{\eta} = 0{\cdot}548$, $\tilde{\eta} = 0{\cdot}084$; (*b*) $r/d = 1{\cdot}3$, $\bar{\eta} = 0{\cdot}181$, $\tilde{\eta} = 0{\cdot}087$; (*c*) $r/d = 1{\cdot}49$, $\bar{\eta} = 0{\cdot}121$, $\tilde{\eta} = 0{\cdot}079$; (*d*) $r/d = 1{\cdot}8$, $\bar{\eta} = 0{\cdot}041$, $\tilde{\eta} = 0{\cdot}055$.

regions where the intensity of fluctuations in the Raman signal was less than 7 %, where any slight deviations from ideal photodetector statistics became significant. The autocorrelation technique is, however, unaffected by such deviations since the noise introduced by the detector is not correlated.

Although it is not possible to reconstruct a probability distribution exactly from a finite sequence of its moments, Siddall & Diab (1975) have developed a method of obtaining a realistic approximation by maximizing the Shannon entropy function (Shannon 1948). Some examples of probability distribution functions (volume fraction methane) at various locations within the jet, obtained by this method, are shown in figure 4. At the centre-line (figure 4(*a*)) the distribution is fairly close to Gaussian with a slight negative skewness. The distribution broadens with increasing radial displacement until the r.m.s. concentration reaches half the mean value (figure 4(*b*)). At this point, $Q(\eta)$ can no longer be approximated by a Gaussian function, since this would require significant probabilities of obtaining negative concentrations. The distribution at $r/d = 1{\cdot}49$, shown in figure 4(*c*), has become bimodal with a high probability of the concentration being zero. This effect is probably due to intermittency in the flow, with eddies of pure air being convected through the sample volume and is shown up more clearly in figure 4(*d*), for a location close to the extreme edge of the jet. It is for distributions such as those shown in figures 4(*c*) and (*d*) that inaccuracies arise when transforming the mean concentration from volume to mass fraction using only the first term of (12).

4.2. *Axial profiles in the free jet*

(*a*) *Mean concentration decay.* The mean concentration profile along the jet centre-line is shown in figure 5 in terms of both mass and volume fraction, the mass fraction values being calculated using (12). A general form for the axial mean concentration decay, normalized by the inlet value $\bar{\theta}_0$, has been given by Hinze (1959) and Field *et al.* (1967):

$$\bar{\theta}/\bar{\theta}_0 = k_1 d_\epsilon/(z + a_1). \tag{18}$$

The general hyperbolic form of this equation can be deduced from similarity considerations, while Thring & Newby (1953) introduced the concept of an effective diameter d_ϵ ($= d(\rho_0/\rho_a)^{\frac{1}{2}}$) to account for density differences between the jet and ambient fluids. Thus a plot of reciprocal concentration against axial distance should be a straight line with a slope equal to $k_1(\rho_0/\rho_a)^{\frac{1}{2}}$. From figure 5 it can be seen that after the development region this slope continues to increase slightly throughout the near field, an effect previously reported for velocity decay by Wygnanski & Fiedler (1969). The data in the far field region (from 25 diameters onwards) can be accurately described by $k_1 = 4{\cdot}0$ and $a_1 = -5{\cdot}8d$ (solid line, figure 5). Values of the decay constant k_1 reported in the literature range from 4 to 6; the exact value probably depends on the jet configuration used. Also, the use of near field data will tend to produce a higher value; for example the present data from 10 to 30 diameters can be adequately described by a decay constant of 4·7.

The reciprocal of the centre-line mean velocity is also shown for comparison in figure 5, and exhibits similar features. A hyperbolic decay constant of 5·01 characterized the far field, which is in close agreement with a value of $\sim 5{\cdot}05$ obtained from the data presented by Wygnanski & Fiedler (1969).

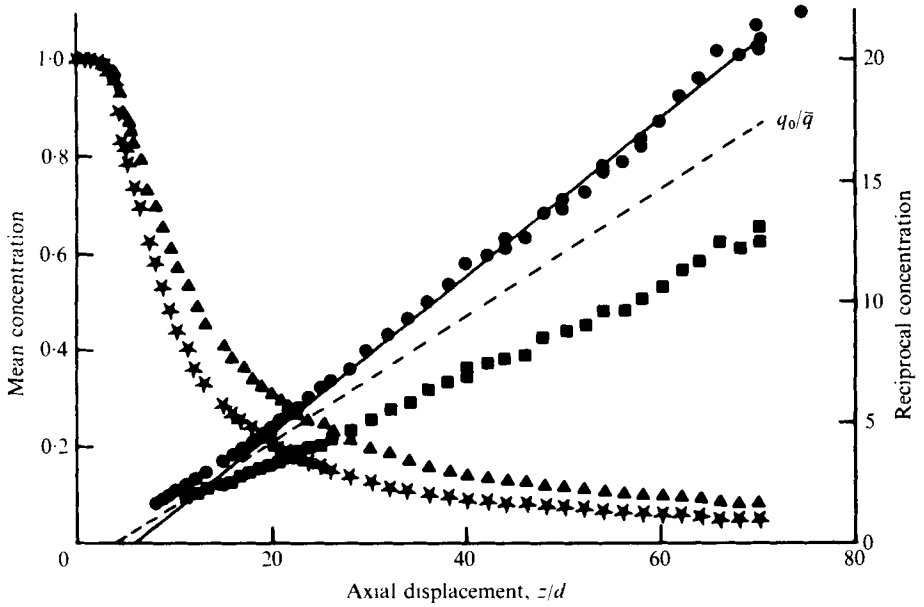

FIGURE 5. Axial decay of mean parameters: ▲, $\bar{\eta}$; ★, $\bar{\theta}$; ■, $1/\bar{\eta}$; ●, $1/\bar{\theta}$.

(*b*) *The second moment of concentration.* The r.m.s. concentration was measured in volume fraction terms by both autocorrelation and from the photon count distributions as described above and converted into mass fraction terms using (14). The centre-line mass fraction r.m.s. concentrations are shown in figure 6; it can be seen that after 10 diameters the decay is hyperbolic, as shown by the linear reciprocal plot. The data were fitted to the function

$$\tilde{\theta} = k_2 d/(z + a_2), \tag{19}$$

with $k_2 = 0{\cdot}86$ and $a_2 = -0{\cdot}8d$.

This equation can be combined with (18) to deduce a limiting value of 28·5 % for the unmixedness, $\xi = (\tilde{\theta}/\bar{\theta})$, when z/d is large. The axial profile of ξ is shown in figure 7 in comparison with the velocity turbulence intensity levels obtained from the optical anemometer. An interesting feature is that, after the rapid increase of unmixedness in the development region, a gradual increase continues and the limiting value of 28·5 % is only approached after 70 diameters. This is because the r.m.s. concentration decay develops to similarity much more rapidly than the mean decay, and hence the asymptotic unmixedness will only be approached at relatively large values of z/d. In contrast, the corresponding velocity function reaches a steady value of approximately 32 % after an axial displacement of 30 diameters, the local value of the fluctuation intensity being everywhere lower for concentration than for velocity. This value for turbulence intensity was somewhat higher than that usually found in air jets. To investigate this further, the axial growth of velocity fluctuations was measured in the jet when the working fluid was air, the flow having the same Reynolds number. The limiting value of turbulence intensity was found to be approximately 27 %, in good agreement with the generally accepted value. It would therefore seem that axial turbulence intensity levels are higher in a jet of natural gas than in equivalent constant density jets.

An alternative method of studying concentration fluctuations has been reported by

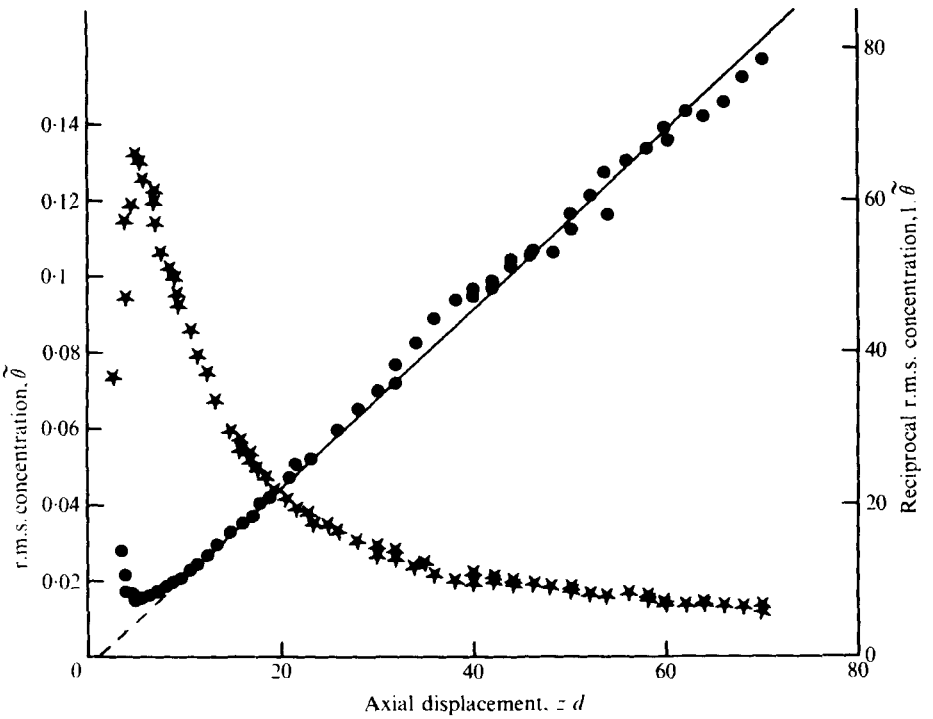

FIGURE 6. Axial decay of r.m.s. concentration: ★, $\tilde{\theta}$; ●, $1/\tilde{\theta}$.

Rosensweig, Hottel & Williams (1961) and Becker *et al.* (1967). Here light scattered from smoke particles introduced into the flow can be used as a measure of the local instantaneous concentration, although allowance has to be made for the inertia of the particles and for any tendency to evaporate or coagulate. Some unmixedness results obtained using this method are shown in figure 7 for a jet of diameter 6·35 mm and Reynolds number 54 000. These results show that the unmixedness has not achieved a steady value by 35 diameters, which is in agreement with our observations. These authors deduced an equilibrium value of 22·2 % for the unmixedness in the ultimate self-preserving state. We may therefore tentatively conclude that (*a*) unmixedness levels are generally lower than turbulence intensity values, and (*b*) both quantities are smaller for constant density flows compared with positively buoyant jets.

We have also compared our data with measurements of temperature fluctuations obtained in heated air jets by Corrsin & Uberoi (1949) and Wilson & Dankwerts (1964). Although there are differences in detail, both indicate values for the maximum temperature fluctuation intensity of approximately 18 %. However, more recent work by Antonia *et al.* (1975) suggests a value of 25·5 % at 59 diameters. It does not therefore seem possible to draw any firm conclusions as to the relative magnitude of concentration and temperature intensities at this stage.

(*c*) *Higher moments of the concentration distributions.* Measurements of the normalized third and fourth central moments of the concentration probability distributions (i.e. skewness and kurtosis factors) are shown in figure 8. These results show that the centre-line distributions are negatively skewed with a constant value of approximately $-0{\cdot}35$ from 20 diameters onwards although some variation may be present in

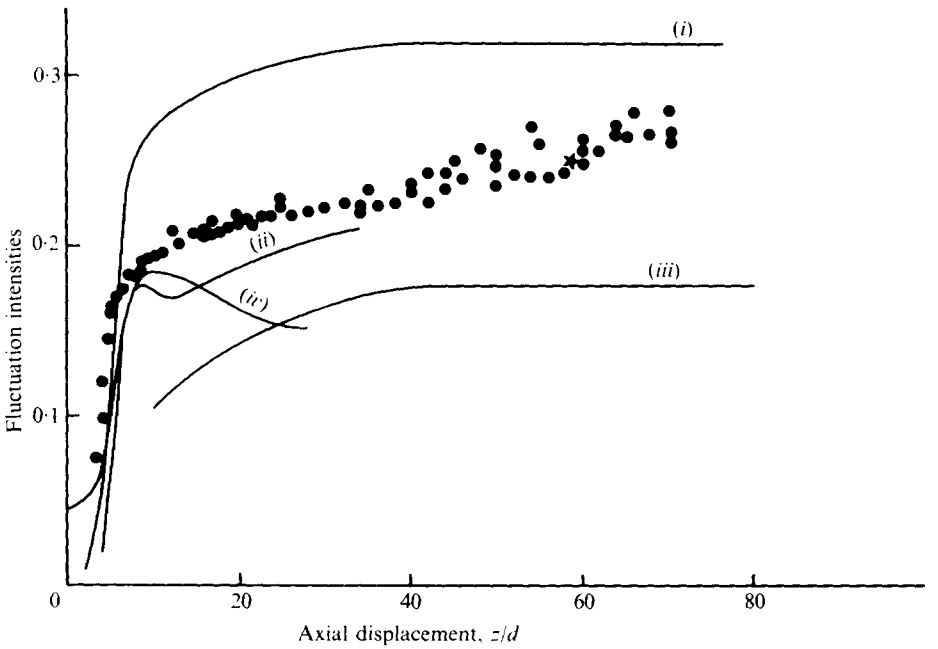

FIGURE 7. Axial variation of fluctuation intensities: ●, present work; ★, Antonia *et al.*, temperature; (*i*) velocity (authors); (*ii*) Becker *et al.* concentration (air jet); (*iii*) Wilson & Dankwerts, temperature; (*iv*) Corrsin & Uberoi, temperature.

the development region. The distributions are slightly peaked, but flatten with axial distance, the kurtosis decreasing slowly from about 3·3 at 15 diameters to about 3·1 at 70 diameters.

We have not been able to compare these results directly with other measurements on concentration, but for temperature probability distributions on the centre-line of heated air jets Venkataramani *et al.* (1975) report a skewness of $-0{\cdot}3$ and kurtosis of 3·07 at 15 diameters downstream in a 22·5 mm diameter jet. Antonia *et al.* (1975) found a skewness factor of $-0{\cdot}5$ and a kurtosis of approximately 3 at a location 59 diameters downstream in a 20·3 mm diameter jet. Corresponding skewness factors for velocity are found to be close to zero in the self-preserving region (e.g. Wygnanski & Fiedler 1969).

An interesting theoretical study of the evolution of the probability density function of the temperature field in a turbulent heated free jet has been carried out by Dopazo (1975) using similarity arguments. His results are based on a conditionally normal probability distribution at a reference location ten diameters downstream on the centre-line, and he predicts an increase in the skewness factor to $+0{\cdot}092$ at 30 diameters followed by an imperceptible decrease. However, as corresponding experimental values of skewness are always found to be negative on the centre-line, these predictions should presumably be taken to indicate relative behaviour rather than absolute values. No conclusions concerning such a small variation can be drawn from our data, but the prediction of constant skewness in the far field is supported.

(*d*) *The integral scale of concentration fluctuations.* The axial variation of the integral time scale $\mathscr{T}$, obtained by autocorrelation, is shown in figure 9(*a*). This time scale has been combined with the local axial mean velocity $\bar{q}$, using Taylor's hypothesis, to

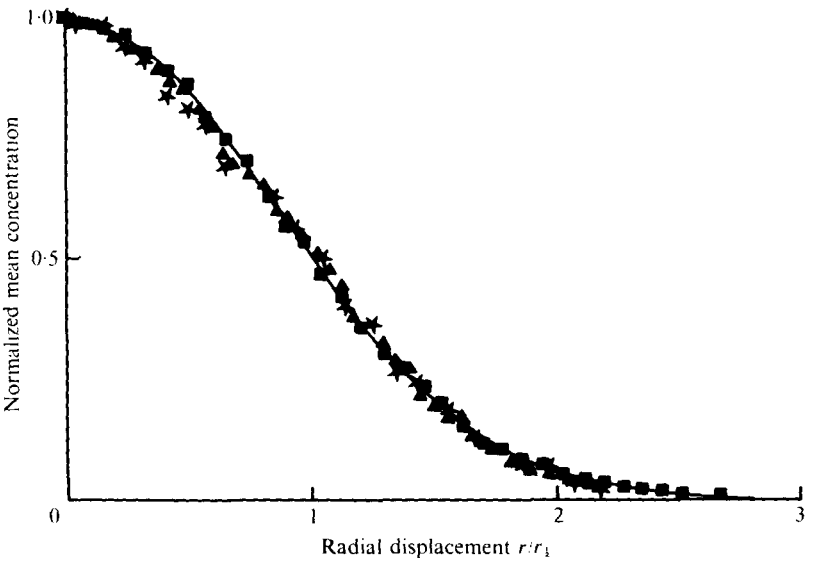

FIGURE 10. Radial profiles of mean concentration: ■, $z/d = 20$; ▲, $z/d = 30$; ★, $z/d = 40$.

Since the velocity decays in a hyperbolic manner, analogous to (18) defined by the constants k_4 and a_4, and since $(z+a_4) \approx (z+a_3)$ in the far field, then

$$\Lambda = \mathscr{T}\bar{q} = k_3 k_4 (z+a_3), \tag{21}$$

which implies that the integral length scale is independent of density ratio provided that the form of (20) is correct.

4.3. *Radial profiles in the jet*

(*a*) *Mean concentration.* The normalized profiles of mean mass fraction concentration, $\bar{\theta}/\bar{\theta}_c$, where $\bar{\theta}_c$ is the centre-line value of the mean concentration, are shown in figure 10, for various axial locations, the radial displacement being normalized using $r_{\frac{1}{2}}$, the distance at which the concentration had decayed to half its centre-line value. These half-widths at various distances downstream are shown in table 1, together with those of Becker *et al.* (1967). It can be seen that the profiles have a similar shape when normalized in this manner, the variation in half-width being at most 3 %. These radial profiles could be accurately described, for $r/r_{\frac{1}{2}} \leqslant 2{\cdot}2$, in terms of the following Gaussian function:

$$\bar{\theta}/\bar{\theta}_c = \exp\{-D(r/z)^2\}, \tag{22}$$

where r/z was chosen rather than $r/(z+a)$ owing to small variations in the estimated virtual origin throughout this region. Taking an average value for $r_{\frac{1}{2}}/z$ as 0·097, then D is found to be 73·6 (solid line in figure 10). It should be noted that a slightly different value for the constant D will be obtained if the virtual origin is included in (22). The close agreement of the $r_{\frac{1}{2}}/d$ values reported here and those given by Becker *et al.* (1967) for an air jet suggests that the jet half-angle is independent of the density ratio between jet and ambient fluids.

z/d	$r_{\frac{1}{2}}/d$	$r_{\frac{1}{2}}/z$	$r_{\frac{1}{2}}/d$ (Becker *et al.*)
10	0·97	0·0972	0·98
20	1·95	0·0975	1·87
30	2·95	0·0982	2·93
40	3·81	0·0952	3·98

TABLE 1

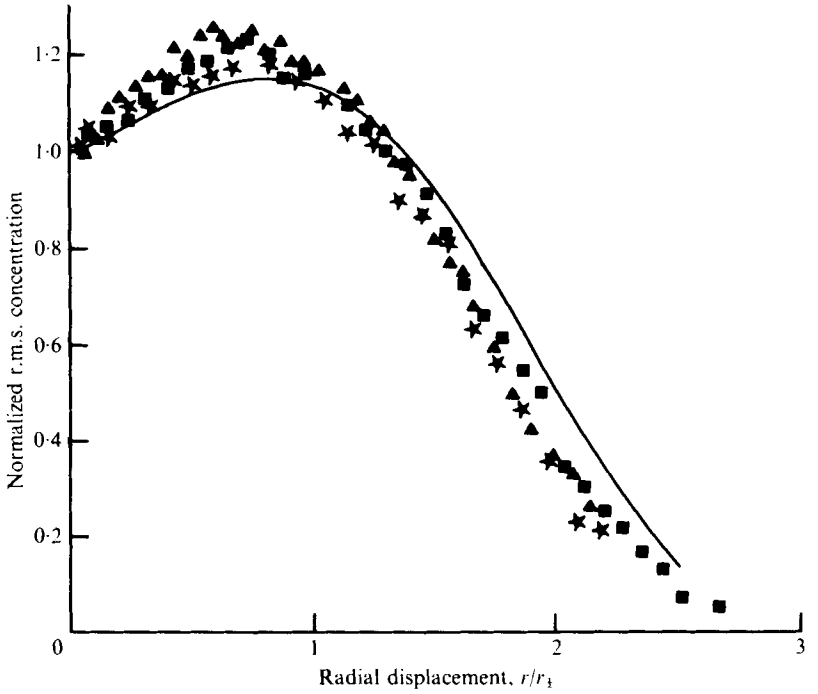

FIGURE 11. Radial profiles of r.m.s. concentration: ■, $z/d = 20$; ▲, $z/d = 30$; ★, $z/d = 40$; —, Becker *et al.*

(*b*) *Second moment of concentration.* The r.m.s. (mass fraction) profiles of $\tilde{\theta}/\tilde{\theta}_c$ are presented in figure 11, the radial displacement being normalized by the mean concentration half-width $r_{\frac{1}{2}}$. The results show that the r.m.s. concentration reaches a maximum, approximately 22 % higher than the centre-line value, at $r/r_{\frac{1}{2}} = 0{\cdot}7$, and are in close agreement with those of Antonia *et al.* (1975) for the corresponding r.m.s. temperature value in a heated air jet. Also shown are r.m.s. concentration results obtained by Becker *et al.* (1967) using the smoke scattering technique in an air jet, which are in turn representative of other results using the same technique (Shaughnessy & Morton 1977; Rosensweig *et al.* 1961). These profiles for constant density jets are somewhat broader, and exhibit a slightly lower maximum value of 16 % in excess of the centre-line level. This effect is possibly analogous to the lower levels of fluctuation intensity observed on the centre-line of constant density jets.

(*c*) *Higher moments of the concentration fluctuations.* The radial profiles of the

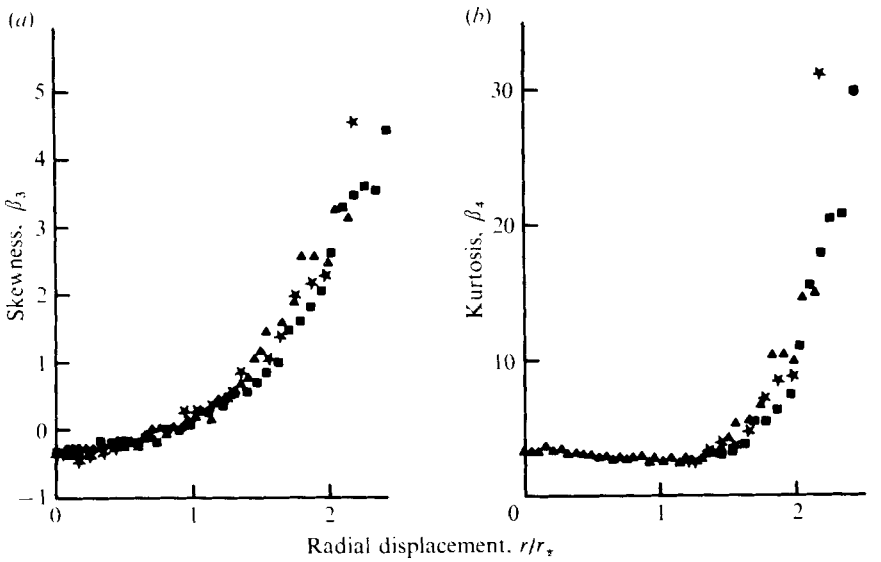

FIGURE 12. Radial profiles of (*a*) skewness and (*b*) kurtosis factors: ■, $z/d = 20$; ▲, $z/d = 30$; ★, $z/d = 40$.

skewness factor β_3, and kurtosis β_4, of the concentration probability distributions are shown in figure 12 for axial locations 20, 30 and 40 diameters downstream from the jet source. The slight negative skewness at the centre-line has already been discussed; the distribution becomes positively skewed at $r/r_{\frac{1}{2}} \simeq 0{\cdot}8$ and thereafter the skewness increases until a value of approximately 4 is reached at the edge of the jet. The kurtosis is close to the Gaussian value until the effects of intermittency become significant at $r/r_{\frac{1}{2}} \simeq 1{\cdot}5$, after which β_4 rapidly increases to values in excess of 30. It should be noted that in the intermittent regions, the moments presented are insufficient to characterize the distributions. However, additional higher moments can be readily obtained from (6), and the reconstructions shown in figure 4 were based on the first six moments.

Although there is little published information available on the higher moments of concentration fluctuation distributions, the results do show good agreement with measurements of higher moments of temperature fluctuations in a heated air jet made by Antonia *et al.* (1975). These authors found that the skewness becomes positive at $r/r_{\frac{1}{2}} = 0{\cdot}8$, and both moments attain high values ($\beta_3 \sim 5$) and ($\beta_4 \sim 20$) at the edge of the jet. This transition to positive skewness is to be expected, since scalar quantities cannot have negative values (i.e. the probability density function cannot exist in this region). Therefore, when the standard deviation exceeds about 40 % of the mean (as occurs at $r/r_{\frac{1}{2}} = 0{\cdot}8$), the distribution must become positively skewed, extending further to the right of the mean than to the left. Furthermore, it seems reasonable to suggest that, for the fluctuation intensity to exceed $\sim$ 80 %, a high probability of zero concentration is necessary, as may arise in the intermittent regions of the flow. Antonia *et al.* (1975) observed that if the effects of such intermittency were removed by conditional sampling, the higher moments of the distributions remained closer to the Gaussian values across the whole jet width, although there was still a transition to positive skewness at $r/r_{\frac{1}{2}} \simeq 0{\cdot}8$.

5. Conclusions

A method has been described which enables spectral information and the moments of the probability density distribution function to be determined in a concentration field. Results obtained using this method, which is based on an analysis of Raman scattered laser light, illustrate that, although the mean values are fairly close to mean scalar distributions in other turbulent jet flows, there are significant differences in the fluctuation intensities.

This paper is published by permission of the British Gas Corporation.

Appendix. List of symbols

A	constant of proportionality
a_i	displacement of virtual origin
b	background count rate
C	transmission loss coefficient
D	radial profile constant
d	orifice diameter
d_e	effective orifice diameter
E	power spectral density function
G	photon correlation function
I	light intensity
K	Raman count rate for 100 % natural gas
k_i	constant in axial variation equations
N	molecular number density
n	photon counts
n_s	factorial moments
P, p	probability density distribution functions
Q	probability density function for volume fraction concentration
$\bar{q}$	axial component of mean velocity
R	autocorrelation function
r	radial co-ordinate
$r_{\frac{1}{2}}$	profile half-width
T	time interval
W	integrated light intensity
z	axial co-ordinate
β_3	skewness parameter ($= \mu_3/\mu_2^{\frac{3}{2}}$)
β_4	kurtosis parameter ($= \mu_4/\mu_2^2$)
ϵ	quantum efficiency
ξ	unmixedness
η	instantaneous volume fraction concentration ($= \bar{\eta} + \eta'$)
θ	instantaneous mass fraction concentration ($= \bar{\theta} + \theta'$)
Λ	Eulerian integral length scale
μ_j	jth central moment of a probability distribution
ν	frequency

ρ_0, ρ_a densities of natural gas and air respectively
σ Raman scattering cross-section
τ delay time co-ordinate
$\mathscr{T}$ Eulerian integral time scale
Ω solid angle

Subscripts

o orifice conditions
c centre-line conditions

Overscores

$-$ average value
$\sim$ root-mean-square value

REFERENCES

Antonia, R. A., Prabhu, A. & Stephenson, S. E. 1975 Conditionally sampled measurements in a heated turbulent jet. *J. Fluid Mech.* **72**, 455–480.

Becker, H. A., Hottel, H. C. & Williams, G. C. 1967 The nozzle fluid concentration field of the round turbulent free jet. *J. Fluid Mech.* **30**, 285–303.

Bédard, G. 1967 Analysis of light fluctuations from photon counting statistics. *J. Opt. Soc. Am.* **57**, 1201–1206.

Birch, A. D., Brown, D. R., Dodson, M. G., Thomas, J. R. 1975*a* The determination of gaseous concentration fluctuations using Raman photon correlation spectroscopy. *J. Phys. D. Appl. Phys.* **8**, L 167–170.

Birch, A. D., Brown, D. R. & Thomas, J. R. 1975*b* Photon correlation spectroscopy and its application to the measurement of turbulence parameters in fluid flows. *J. Phys. D. Appl. Phys.* **8**, 438–447.

Corrsin, S. & Uberoi, M. S. 1949 Further experiments on the flow and heat transfer in a heated turbulent air jet. *N.A.C.A. Tech. Note* no. 1865.

Dopazo, C. 1975 Probability density function approach for a turbulent axisymmetric heated jet – centreline evolution. *Phys. Fluids* **18**, 397–404.

Fenner, W. R., Hyatt, H. A., Kellam, J. M. & Porto, S. P. S. 1973 Raman cross-sections of some simple gases. *J. Opt. Soc. Am.* **63**, 73–77.

Field, M. A., Gill, D. W., Morgan, B. &. Hawksley, P. G. W. 1967 Combustion of pulverised coal. *British Coal Utilisation Research Association.* Leatherhead, England.

Grant, A. J., Jones, J. M. & Rosenfeld, J. L. J. 1973 Orderly structure and unmixedness in lifted jet diffusion flames. *Combustion Institute European Symposium*, pp. 548–552. Academic Press.

Hartley, D. L. 1974 Application of laser Raman scattering to the study of turbulence. *A.I.A.A. J.* **12**, 816–821.

Hinze, J. A. 1959 *Turbulence.* McGraw-Hill. (See also 2nd edn, 1975.)

Jakeman, E. 1973 *Photon Correlation and Light Beating Spectroscopy* (ed. H. Z. Cummings & E. R. Pike), pp. 75–149. Plenum.

Long, V. D. 1963 Estimation of the extent of hazardous areas around a vent. *2nd Symposium on Chemical Process Hazards*, pp. 6–14.

Mandel, L. 1959 Fluctuations of photon beams: the distribution of the photo-electrons. *Proc. Phys. Soc.* **74**, 233–243.

Meltzer, D. & Mandel, L. 1970 Determination of intensity correlation functions from photo-electric counting distributions. *I.E.E.E. J. Quantum Electronics* **QE–6**, 661–668.

Pike, E. R. 1969 Photon statistics. *Nuovo Cimento* **1**, 277–314.

RIBEIRO, M. M. & WHITELAW, J. H. 1974 Statistical characteristics of a turbulent jet. *Imperial College of Science and Technology Report* no. HTS/74/19.

ROSENSWEIG, R. E., HOTTEL, H. C. & WILLIAMS, G. C. 1961 Smoke-scattered light measurements of turbulent concentration fluctuations. *Chem. Engng Sci.* **15**, 111–129.

SHANNON, G. E. 1948 A mathematical theory of communication. *The Bell System Technical J.* **27**, no. 3.

SHAUGHNESSY, E. J. & MORTON, J. B. 1977 Laser light-scattering measurements of particle concentration in a turbulent jet. *J. Fluid Mech.* **80**, 129–148.

SIDDALL, J. N. & DIAB, Y. 1975 The use in probabalistic design of probability curves generated by maximising the Shannon entropy function constrained by moments. *Trans. A.S.M.E., J. Engng Indust.* **97**, 843–852.

THRING, M. W. & NEWBY, M. P. 1953 Combustion length of enclosed turbulent jet flames. *4th Symposium (International) on Combustion*, pp. 789–796. Baltimore: Williams & Wilkins.

TOBIN, M. C. 1971 *Laser Raman Spectroscopy*. John Wiley and Sons, New York.

VENKATARAMANI, K. S., TUTU, N. K. & CHEVRAY, R. 1975 Probability distributions in a round heated jet. *Phys. Fluids* **18**, 1413–20.

WIDHOPF, G. F. & LEDERMAN, S. 1971 Specie concentration measurements utilising Raman scattering of a laser beam. *A.I.A.A. J.* **9**, 309–316.

WILSON, R. A. M. & DANCKWERTS, P. V. 1964 Studies in turbulent mixing – II. A hot-air jet. *Chem. Engng Sci.* **19**, 885–895.

WYGNANSKI, I. & FIEDLER, H. 1969 Some measurements in the self-preserving jet. *J. Fluid Mech.* **38**, 577–612.